MULTISTATION BUNDLE ADJUSTMENT WITH A MACHINE VISION PARALLEL CAMERA SYSTEM - AN ALTERNATIVE TO THE PERSPECTIVE CASE FOR THE MEASUREMENT OF SMALL OBJECTS

M. Rova, S. Robson, M.A.R. Cooper

Department of Civil, Environmental and Geomatic Engineering, University College London, Gower Street, London, WC1E 6BT UK - mrova@cege.ucl.ac.uk, -srobson@cege.ucl.ac.uk,- m.a.r.cooper@ucl.ac.uk

Commission V, WG V/1

KEY WORDS: Calibration, Orientation, Measurement, Bundle Adjustment, Parallel Projection

ABSTRACT:

Photogrammetric measurement and modelling procedures are dependent on accurate camera calibration and orientation. The accuracy of image-based registration and texture mapping approaches can be deficient up to the underlying camera projection. In the case of small objects an alternative to the conventional central projection model can be to use parallel projection cameras which deliver small volumes under constant sampling. Cameras of variant geometries have been studied by the computer vision community; but they impose algorithmic assumptions into the projective model which can degrade the stability of the solutions. This paper proposes the development of a multiphoto bundle adjustment for parallel cameras based on an analytical mathematical model with quality assessment. The model is treated for multiphoto situations; the image to object space correspondence is established under invariant scaling through the pseudo exterior orientation elements; the camera is calibrated for the first term of the radial lens distortion. Initialization is recovered indirectly through perspective-based strategies and direct solutions based on orthographic projection. The algorithmic stability is verified with true parallel projection image sequences of 3D calibration structures captured with a telecentric camera system within controlled calibration conditions.

1. INTRODUCTION

Accurate 3D measurements are fundamental prerequisites in close range engineering and archaeological applications. Image based approaches for the generation of textured 3D models are based on stereo or multi-image matching strategies (Remondino and Zhang, 2006). In a larger scale alternative techniques combine images with laser scan range data; the accuracy achieved is dependent on the registration and texture mapping methods (El Hakim et. al., 1998). The selected approach is constrained by the object geometry, texture and the metric requirements. Existing algorithmic approaches for image-based registration require that the cameras are calibrated within geometrically strong image networks. In industrial metrology applications cameras are routinely calibrated based on established bundle adjustment strategies with self - calibration (Brown 1974; Granshaw, 1980). Cameras are calibrated prior or together with the 3D measurement of the objects to be modelled based on signalized or natural features of interest and requiring manual or semi-automated point measurement. Purpose designed volumetric or planar testfields are imaged to satisfy algorithmic assumptions within both photogrammetric and computer vision communities (Triggs et. al., 2000; Clarke and Fryer 1998; Fraser, 2001; Gruen and Beyer, 2001). When the imaging conditions are limited to a few focal lengths from the object of interest the central perspective model introduces significant geometric and radiometric distortions; extended camera models account for variations in distortions with object distance (Shortis et. al., 1996).

Computer vision recovers the image to object space correspondence linearly. Variant cameras geometries are treated with the homogeneous determination of the involved matrices; linear algorithms impose algorithmic assumptions into the projective model which can deteriorate the stability of the solutions. Parallel projection establishes the image to object space correspondence under invariant scaling; hence it eliminates perspective distortions but it is limited by its field of view. Such systems fall into the generalized category of affine cameras which are closer to the Euclidean reconstruction and are mathematically simple to implement due to their linearity. Geometric approaches are typically based on local coordinate frame methods (Koenderink and Van Doorn, 1991). Tomasi and Kanade, 1992 propose a non-local coordinate frame method that utilizes all the available scene points but rank considerations have to be considered. Coordinate datums are defined as the centroid of the cluster of targets. Shapiro, 1995 follows the extended m-view approach based on the singular value decomposition of the involved matrices. A detailed review on the affine analysis from image sequences can be found in the literature (Shapiro, 1995). Alternative approaches initialize orientation procedures (Kyle, 2004) and introduce an orthogonality constraint into the affine model independently on approximate values (Ono et. al., 2004) or propose a unified approach for both perspective and orthographic cameras based on collinearity condition to map textures onto planar polygons (Weinhaus and Devich, 1999).

This paper focuses on the calibration of sequentially acquired images under parallel projection within a bundle adjustment procedure. The mathematical model has been formed for the multiphoto case and was treated as the non-linear equivalent of the standard perspective - based bundle method. In the absence of the projection centre the pseudo exterior orientation parameters link the image to the object space measurements through the 2D projective translations, the global image scale and the 3D orientation angles. A simplified interior orientation model takes into account the first term of the radial lens distortion. The model is initialized indirectly through perspective based resection procedures and direct parallel projection solutions by back-substitution. The datum ambiguity problem is accommodated by either the inner or external constraints methods (Cooper, 1987).

In photogrammetric terms, prior concern is to assess the behaviour of a unified parallel - based multistation bundle adjustment in terms of checking the stability of the orientation parameters (interior and exterior); mainly to assess the metric recovery when measuring small 3D structures. The algorithm was validated with real convergent image sequences acquired with a true physical parallel geometry imaging system. The experimental set up and measurements were conducted at the UCL calibration laboratory.

2. MATHEMATICAL MODEL

Parallel projection falls into the generalized category of the affine camera. It corresponds to a projective camera with its projection centre at infinity (Hartley and Zisserman, 2004). Weak perspective projection can be derived from perspective when the object size is small compared to the imaging range. The standard perspective equations become linear; parallel projection can then be conceived as a double projection. All the object points are projected orthographically onto a plane which goes through the depth of the object's centroid followed by a perspective projection onto the image plane under uniform scaling (Xu and Zhang, 1996).

The 2D image vector x (observations) is linked with its 3D equivalent vector X (object space) through a (2x3) magnification matrix M (=sR) and a 2D translation vector t. The mathematical model in its simple form is given by Equations 1 and 2 in vector and matrix terms respectively.

$$\underset{(2x1)}{x} = s \underset{(2x3)}{R} \underset{(3x1)}{X} + \underset{(2x1)}{t} \tag{1}$$

$$\begin{bmatrix} x \\ y \end{bmatrix} = s \begin{bmatrix} r_{11} & r_{12} & r_{13} \\ r_{21} & r_{22} & r_{23} \end{bmatrix} \begin{bmatrix} X \\ Y \\ Z \end{bmatrix} + \begin{bmatrix} tx \\ ty \end{bmatrix} \tag{2}$$

$$R = \begin{bmatrix} r_{11} & r_{12} & r_{13} \\ r_{21} & r_{22} & r_{23} \\ r_{31} & r_{32} & r_{33} \end{bmatrix}$$

x,y : image coordinates
s : image scale
r_{ij} : rotation matrix elements
X, Y, Z : object space 3D coordinates
tx, ty : 2D projective translations

The projection centre is located at infinity. The translation vector t expresses the projective equivalents of the principal point components but it is locally variant through the image sequence. Whilst, full self calibration would require the inclusion of the lens distortions polynomials (radial and tangential) together with affinity and orthogonality parameters; it is the physical algorithmic stability which judges the full model formulation. Figure 1 illustrates a convergent image network that intersects the parallel lines of sight under invariant scale.

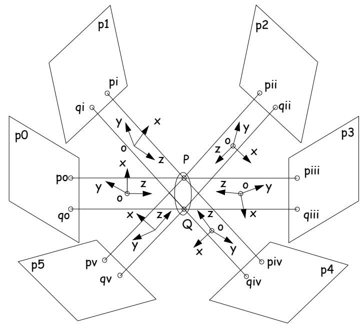

Figure 1 Multiphoto intersection - parallel case.

3. BUNDLE ADJUSTMENT

The developed approach treats the basic parallel projection mathematical model within a rigorous multiphoto bundle adjustment with the aim of allowing both parallel and perspective imaging systems to exist within the same photogrammetric network.

The key issue is the choice of the physical parameters to be estimated. The model includes the basic camera model parameters taking into account the first term of the radial lens distortion considering minimum distortion based on manufacturers data for the telecentric optics deployed. Next, the parameters are grouped according to their type to assist the population of the required arrays. Parameters are grouped together as pseudo exterior orientation parameters (projective equivalents of the principal point components- tx, ty, global scale s, 3D rotation angles- omega, phi, kappa) which are image variant, the 3D targets coordinates (X, Y, Z) and additional parameters terms (k_1) (Equation 3). Hence, the system is populated with the five exterior parameters per image, one for the global scale (one camera) in the designed arrangement, three per target and one for the first radial polynomial term (again per camera). The radial lens distortion is modelled centrally from the computed tx,ty image centre.

$$\begin{bmatrix} x - x^o \\ y - y^o \end{bmatrix}_{ji} = \begin{bmatrix} \frac{\partial x}{\partial t_x} & \frac{\partial x}{\partial t_y} & \frac{\partial x}{\partial s} & \frac{\partial x}{\partial \omega} & \frac{\partial x}{\partial \varphi} & \frac{\partial x}{\partial \kappa} \\ \frac{\partial y}{\partial t_x} & \frac{\partial y}{\partial t_y} & \frac{\partial y}{\partial s} & \frac{\partial y}{\partial \omega} & \frac{\partial y}{\partial \varphi} & \frac{\partial y}{\partial \kappa} \end{bmatrix}_{ji} \begin{bmatrix} \delta t_x \\ \delta t_y \\ \delta s \\ \delta\omega \\ \delta\varphi \\ \delta\kappa \end{bmatrix}_j + \begin{bmatrix} \frac{\partial x}{\partial X} & \frac{\partial x}{dY} & \frac{\partial x}{dZ} \\ \frac{\partial y}{\partial X} & \frac{\partial y}{\partial Y} & \frac{\partial y}{\partial Z} \end{bmatrix}_{ji} \begin{bmatrix} \delta X \\ \delta Y \\ \delta Z \end{bmatrix}_i + \begin{bmatrix} \frac{\partial x}{\partial k_1} \\ \frac{\partial y}{\partial k_1} \end{bmatrix}_{ji} \begin{bmatrix} \delta k_1 \end{bmatrix}_j + \begin{bmatrix} v_x \\ v_y \end{bmatrix}_{ji} \tag{3}$$

Considering j photos and i targets in a network configuration the over determined linear system of equations is processed in a least squares approach that minimizes the reprojection error according to the standard Gauss Markov model. The problem is weighted considering that the quality of the image observations is defined with a standard deviation of 0.5μm which is typical for close range perspective imaging with the Kodak Megaplus sensor used for subsequent tests. The system is solved iteratively until the correction vector satisfies the convergence criteria. The orientation tolerance was set to 0.1 x σ and the targets and additional parameters to 0.04 x σ as appropriately.

For the purposes of these tests effective starting values required to intiate the bundle adjustment process were computed within a photogrammetric measurement system (Vision Measurement System, VMS, Robson S. and Shortis M.). To avoid geometric degeneracies introduced by planar configurations control targets in a 3D volume arrangement have been used. Initialization is implemented by a modified Zeng and Wang closed form resection procedure assuming that perspective projection with a very long focal length is a good initial approximation to a parallel projection (Zeng and Wang, 1992). An initial space resection, again using a long focal length, is computed to refine the starting values. Indirect 3D orientation angles recovery is sensitive to the 3D targets geometry. Next, given the knowledge of the partial exterior orientation together with the coordinates of the 3D control targets, the 2D projective translations are recovered from the initialized parallel projection model by back-substitution.

To avoid the datum ambiguity problem the network can be externally constrained based on the 3D coordinates of all control targets given the knowledge of their stochastic model. Alternatively the datum is defined by the centroid of the control targets by setting the minimum required constraints of a 3D similarity transformation (3 translations, 3 rotations and 1 scale) by the inner constraints method assuming a normalized precision for the 7 additional equations. Inner constraints are a convenient method for removing any deficiencies coming from the control data to provide a minimum constraints datum that minimizes the trace of the dispersion matrix. An indicator of the quality of the adjustment is obtained by the computation of the a-posteriori standard deviation and through analysis of the scaled covariance matrix to check the precision of the estimated parameters and any potential correlations in the model. Figure 2 illustrates the structure of the design and normals matrices for a subset of photos and targets (external constraints method).

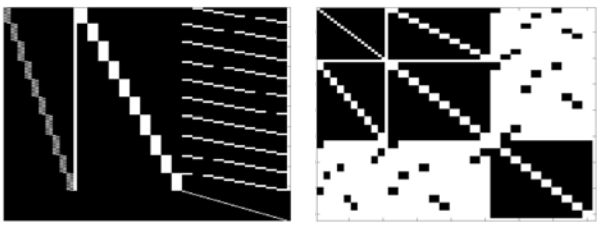

Figure 2 Parallel camera arrangement for 10 photos & 10 control targets (tx_j, ty_j, s, ω_j, φ_j, κ_j, X_i, Y_i, Z_i, k_1) design & normals matrices (external constraints).

4. ALGORITHM ASSESSMENT

The algorithm was tested with real parallel projection convergent image sequences acquired with a telecentric camera system under controlled conditions. The system consists of a MVO double sided telecentric lens (nominal scale 0.16) fitted onto a “C” mount Kodak Megaplus ES 1.0 monochrome camera 1008 x 1018 pixels (pixel size 9 μm). The camera’s field of view is 40 mm and its imaging range 175 mm. Additional sets were captured with a more conventional wide angle retrofocus Fujinon lens (focal length = 12.5mm) fitted onto a similar camera body.

Three purpose - built calibration structures were constructed, of a few centimetres magnitude, with signalized circular artificial retrotargets and white dots of 2 mm diameter and 0.9 mm respectively. The targets were designed in order to achieve distinctive point measurements at the very close range; their diameter (0.9 mm in object space) is equivalent to 16 pixels under parallel projection and 7 pixels under perspective (image space) (Figure 3).

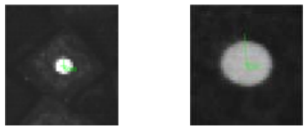

Figure 3 Sample - Perspective & parallel image targets – Range 175mm - 0.9 mm diameters (magnification 40x).

These were imaged simultaneously with both the perspective and parallel camera systems by introducing controlled rotations at regular intervals based on an optical turntable. Figure 4 illustrates the combined imaging system with the perspective and parallel camera models.

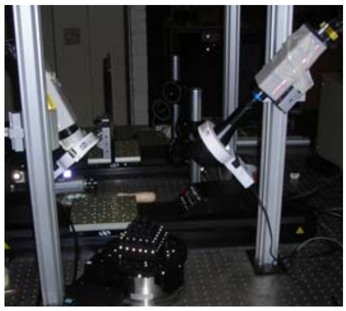

Figure 4 Camera system.

To test the algorithm a homogeneous processing framework was selected for the three datasets. First the perspective camera was pre-calibrated within a self calibrating bundle adjustment procedure (based on a ten-parameter extended model) with the inner constraints method and the introduction of linear scalar constraints (VMS). Having pre-measured the calibration objects the local datum was defined implicitly through perspective. This resulted in a measurement precision of 8 μm (object space) with a relative precision for the network of 1:27,000. The generated point data were used to run the algorithmic verification of the parallel based bundle adjustment; noting that the figures above define the quality of the input data to the parallel network (Figure 5). The accuracy assessment was provided by comparing output distances between targets with independent digital calliper measurements.

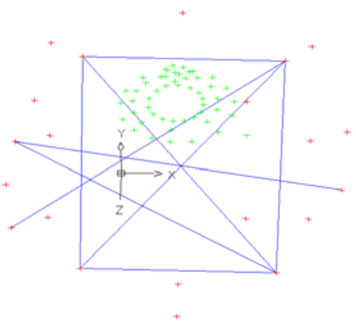

Figure 5 Calibration structure I - features (red = initial control, green = tie, blue = scale).

4.1 Calibration Structure I

The first dataset was composed of 17 images in a convergent wide separated arrangement and viewing 15 control targets (Figure 6). The imaged targets were measured with a weighted centroid method but their 2 mm diameter targets (36 pixels in image space) in this case degrade the overall network precision.

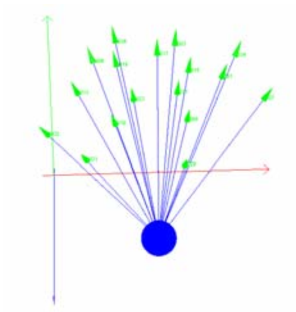

Figure 6 Calibration structure I –Parallel image network geometry.

The algorithm converged at the third iteration with a σ_o of 6.0 indicating a clear misjudgement on the input target precision (50 µm). The bundle adjustment misclosure was 2/10 of a pixel (6 µm on image space) and the targets were coordinated with an rms of 24 µm for both external and inner methods. The camera was calibrated with a scale of 0.1657 and the first term of the radial lens distortion polynomial (Table 7).

	External	Inner
scale	0.1657	0.1657
k_1 x e-004	2.0241	2.0242
observations	555	517
unknowns	132	132
dof	423	385
iterations	3	3
σo	6.3	6.5
$residuals_{xy}$	2 µm	2 µm
stdev	121.3 µm	439.1 µm

Table 7 Calibration Structure I
Bundle Adjustment 17 photos, 15 control targets

4.2 Calibration Structure II

The second dataset is the most optimum in terms of network geometry. In this case 30 parallel geometry images were taken in a wide two ring arrangement viewing 18 control targets (Figures 8 and 9).

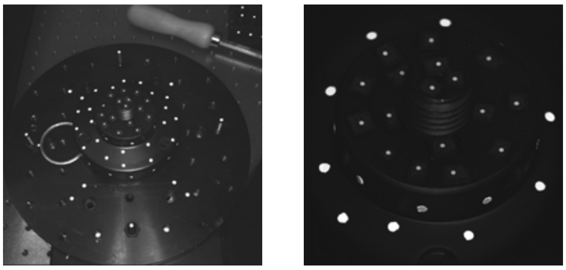

Figure 8 Calibration structure II –
Perspective & parallel views - range 175mm.

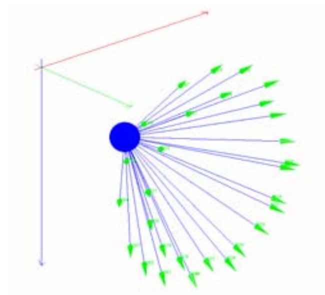

Figure 9 Calibration structure II –Parallel image network geometry.

The camera was calibrated with a scale of 0.1614; the triangulation misclosure was 1/10 of a pixel (0.6 µm). The targets were coordinated with an rms of 5 µm for both external and inner constraints and a precision of 32 µm and 102 µm per method. The aposteriori σ_o was nearly one; which satisfies the designed stochastic model (Table 10). The accuracy was approximately 0.4 mm given the measurement of five true slope distances.

	External	Inner
scale	0.1614	0.1614
k_1 x e-004	1.6762	1.6761
observations	980	933
unknowns	206	206
dof	774	727
iterations	3	3
σo	1.8	1.8
$residuals_{x,y}$	0.6 µm	0.6 µm
stdev	31.6 µm	102.0 µm

Table 10 Calibration Structure IIBundle Adjustment
30 photos, 18 control targets

4.3 Calibration Structure III

The third dataset (Table 13) behaves similarly to the previous two but the targets coverage within the image format is more complete; hence there is a greater confidence on the recovery of interior geometry. Here 24 images and 20 control targets were captured with a two ring network configuration (Figures 11 and 12). The calibrated image scale was 0.1616. The overall quality degradation as opposed to the second image - set can be attributed to the network geometry. To assess the accuracy nine check distances were measured between selected targets on the object with a calliper. The mean discrepancy between the bundle adjustment output and the truth data was 0.11 mm.

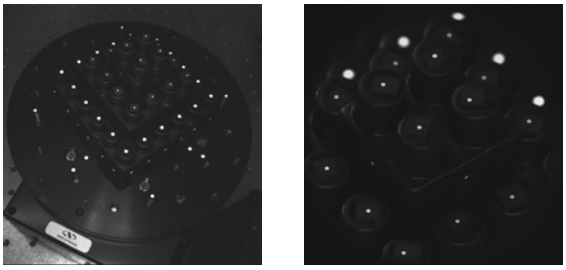

Figure 11: Calibration structure III –
Perspective & parallel views - range 175mm.

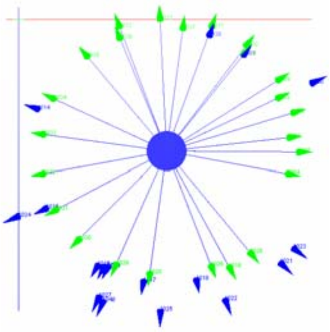

Figure 12 Calibration structure III –
Parallel image network geometry.

	External	Inner
scale	0.1616	0.1616
k_1 x e-005	3.7280	3.7095
observations	604	551
unknowns	182	182
dof	422	369
iterations	3	3
σo	2.6	2.7
residuals_{xy}	0.7 μm	0.7 μm
stdev	43.7μm	134.9μm

Table 13 : Calibration Structure IIIBundle Adjustment
24 photos, 20 control targets

4.4 Comparative Orientation Evaluation

Table 14 summarizes the overall precisions for the three sets of data for the external and inner constraints. The elements of the pseudo exterior orientation are recovered with a precision of 15 μm for the 2D translations and 0.0006 degrees for the 3D rotations in the best case (second dataset) the associated precision for the k_1 term was 0.01 μm.

	tx,ty	ω, φ, κ	k_1
Struct I	50 μm	0.0024 deg	0.05 μm
Struct II	15 μm	0.0006 deg	0.01 μm
Struct III	22 μm	0.0005 deg	0.01 μm
	Inner Constraints: stdev		
Struct I	76 μm	0.0012 deg	0.05 μm
Struct II	18 μm	0.0003 deg	0.01 μm
Struct III	23 μm	0.0002 deg	0.01 μm

Table 14 External Constraints: stdev

The radial lens distortions profiles for the three testfields (Figure 15) prove that the parallel camera is calibrated with less than 0.1% pincushion distortion which is 9 μm in the worst case satisfying the lens specifications provided by the manufacturer. The range of curves seen here demonstrate the inconsistency of image format coverage of the measured target image locations; sets 1 and 2 have less coverage with respect to the third one. Correlation checks for both methods for the three data sets suggest a stabilized algorithmic behaviour for both external and inner constraints methods when used under these relatively strong and controlled convergent network geometries.

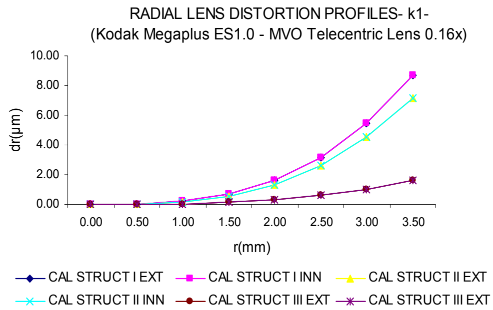

Figure 15 Comparative radial lens distortion profiles (k_1).

5. CONCLUSIONS

The approach presented here implements a multiphoto bundle adjustment for the parallel imaging case. The camera was calibrated with a simplified interior parameters (constant image scale and first term of radial lens distortion) to deliver sub-pixel image measurement precisions of approximately $1/10^{th}$ of a pixel. The algorithm was validated with three controlled datasets and has been proved to converge rapidly with stability comparable to a well configured conventional bundle adjustment process. There are issues open to be answered related to the full interior geometry recovery and choice of more optimal starting values estimations (3D rotation angles and target coordinates) as well as the imaging geometry (inclusion for example of rolled images). The camera, by virtue of its geometrically optimal telecentric lens construction, presents minimal inner distortion but the constant imaging scale combined with the image quality attainable from low cost small physical targets affects the measurement accuracy. However, calibration and metric recovery of true parallel projection image sequences can be advantageous for very close range measurements particularly where texture mapping approaches benefit from constant image magnification.

ACKNOWLEDGEMENTS

The author wishes to acknowledge Dr. Stuart Robson and Prof. Michael Cooper for their guidance in the development of the camera model. This research project is supported by IKY (Greece). Support from the Life, Earth and Environmental Sciences Standing Committee (LESC) of the European Science Foundation made the oral presentation of this paper possible (www.esf.org/lesc).

REFERENCES

Brown, D.C., 1974. Evolution, Application and Potential of the Bundle Method of Photogrammetric Triangulation. International Society for Photogrammetry, Symposium in Stuttgart, Commission III. September 2- 6, 95 pages.

Clarke T. A., and Fryer J. G. 1998. The Development of Camera Calibration Methods and Models. Photogrammetric Record, 16(91): pp. 51-66.

Cooper, M.A.R., 1987. Control Surveys in Civil Engineering. 381 pages.

El Hakim S.F., Brenner, C. and Roth, G., 1998. A multi-sensor approach to creating accurate virtual environments. ISPRS Journal of Photogrammetry & Remote Sensing 53 (1998) pp. 379-391.

Fraser, S.C., 2001. Photogrammetric Camera Component Calibration: A Review of Analytical Techniques. In: Calibration and Orientation of Cameras in Computer Vision. Gruen and Huang (Editors), Springer Series in Information Sciences pp. 95-121.

Granshaw, S.I., 1980. Bundle Adjustment Methods in Engineering Photogrammetry. Photogrammetric Record, Volume 10, Issue 56. pp. 181-207. October 1980.

Gruen, A., and Beyer, H.A, 2001. System Calibration Through Self-Calibration. In: Calibration and Orientation of Cameras in Computer Vision. A. Gruen and T. S. Huang. Springer. pp. 163-193.

Hartley, R. and Zisserman, A., 2004. Camera Models. In: Multiple View Geometry in Computer Vision, pp.156-176. Cambridge University Press. pp. 153-177.

Koenderink J. J., and A. J. Van Doorn, 1991. Affine Structure from Motion. Optical Society of America. Vol 8, No. 2. February 1991. pp. 377-385.

Kyle S., 2004. Using Parallel Projection Mathematics to Orient an Object Relative to a Single Image. The Photogrammetric Record 19(105): 38-50. pp. 38-50.

Ono, T. Akamatsu, S.-I. Hattori, S. 2004. A Long Range Photogrammetric Method with Orthogonal Projection Model. International Archives of Photogrammetry Remote Sensing and Spatial Information Sciences, 2004, Vol 35; Part 3, pp. 1010-1015.

Remondino, F. and Zhang, L., 2006. Surface Reconstruction Algorithms for Detailed Close – Range Object Modelling. International Archives of Photogrammetry, Remote Sensing and Spatial Information Sciences, Vol. XXXVI, part 3, pp. 117-123 ISPRS Commission III Symposium, Bonn, Germany.

Shapiro, L.S., 1995. The Affine Camera and Affine Structure. In: Affine Analysis of Image Sequences. Phd Dissertation. Cambridge University Press, 1995. pp. 9-33.

Shortis, M.R., Robson, S., Short, T., 1996. Multiple Focus Calibration of a Still Video Camera. International Archives of Photogrammetry and Remote Sensing, Vol. 31, Part B5, pp. 534-539, Vienna, July 1996.

Tomasi, C. and Kanade, T., 1992. Shape and Motion from Image Streams: a Factorization Method. Full Report on the Orthographic Case. CMU-CS- 92-104. 36 pages.

Triggs, B., Mc Lauchlan, P., Hartley, R., Fitgibbon, A., 2000. Bundle Adjustment – A Modern Synthesis. Vision Algorithms: Theory and Practice. Editors: B. Triggs, A. Zisserman and R. Szeliski. Springer-Verlag LNCS 1883, 2000. 71 pages.

Weinhaus, F.M., and Devich R.N., 1999. Photogrammetric Texture Mapping onto Planar Polygons. Graphical Models and Image Processing 61, 63-83 (1999), pp. 63-83.

Xu, G., and Zhang Z., 1996. Camera Models and Epipolar Geometry. In: Epipolar Geometry in Stereo, Motion and Object Recognition A Unified Approach. Kluwer Academic Publishers. pp. 7-78.

Zeng, Z., and Wang, X., 1992. A General Solution of a Closed-Form Space Resection. Photogrammetric Engineering and Remote Sensing, 58(3) pp. 327-338.

http://www.geomsoft.com/ - VMS - Vision Measurement System –developed by S. Robson (UCL) and M. Shortis (RMIT University) (accessed Jan. 2008).